Insect Biochemistry and Molecular Biology 90 (2017) 90–100

Contents lists available at ScienceDirect

Insect Biochemistry and Molecular Biology

journal homepage: www.elsevier.com/locate/ibmb

Expressional divergences of two desaturase genes determine the opposite ratios of two sex pheromone components in *Helicoverpa armigera* and *Helicoverpa assulta*

Rui-Ting Li [a, b], Chao Ning [a], Ling-Qiao Huang [a], Jun-Feng Dong [c], Xianchun Li [d], Chen-Zhu Wang [a, b, *]

[a] State Key Laboratory of Integrated Management of Pest Insects and Rodents, Institute of Zoology, Chinese Academy of Sciences, Beijing, China
[b] College of Life Sciences, University of Chinese Academy of Sciences, Beijing, China
[c] College of Forestry, Henan University of Science and Technology, Luoyang, China
[d] Department of Entomology and BIO5 Institute, University of Arizona, Tucson, AZ 85721, USA

ARTICLE INFO

Article history:
Received 30 June 2017
Received in revised form
26 September 2017
Accepted 30 September 2017
Available online 3 October 2017

Keywords:
Helicoverpa armigera
Helicoverpa assulta
Sex pheromone gland transcriptome
Desaturase
Backcross
Fatty acyl reductase

ABSTRACT

The sympatric closely related species *Helicoverpa armigera* and *Helicoverpa assulta* use 97:3 and 7:93 of (Z)-11-hexadecenal and (Z)-9-hexadecenal, respectively, as their sex pheromone to find/locate correct sex mates. Moreover, (Z)-11-hexadecenyl alcohol and (Z)-9-hexadecenyl alcohol are more abundant in the pheromone gland of *H. assulta* than in that of *H. armigera*. To clarify the molecular basis of these differences, we sequenced the pheromone gland transcriptomes of the two species and compared the expression patterns of the candidate enzyme genes involved in the pheromone biosynthetic pathways by FPKM values and quantitative RT-PCR analysis. We found that the desaturase gene *LPAQ* expressed about 70 times higher in *H. armigera* than in *H. assulta*, whereas another desaturase gene *NPVE* expressed about 60 times higher in *H. assulta* than in *H. armigera*. We also observed significantly higher expression of the fatty acyl reductase (FAR) gene *FAR1* and the aldehyde reductase (AR) gene *AR3* in *H. assulta* than in *H. armigera*. Examination of the pheromone glands of the backcross offspring of their hybrids to *H. assulta* showed a positive linear correlation between the expression level of *LPAQ* and the amount of Z11-16:Ald and between the expression level of *NPVE* and the amount of Z9-16:Ald in the pheromone glands. Taken together, these data demonstrate that the expressional divergences of *LPAQ* and *NPVE* determine the opposite sex pheromone component ratios in the two species and the divergent expression of *FAR1* and *AR3* may account for the greater accumulation of alcohols in the pheromone gland of *H. assulta*.

© 2017 Elsevier Ltd. All rights reserved.

1. Introduction

Sex pheromones play an important role in intraspecific communication for mate finding in moths. Their components are usually species-specific fatty acid derivatives produced and emitted by the females from the pheromone gland. The species specificity of pheromones is conferred by the combination and blend ratio of components. Variation of sex pheromone composition can lead to reproductive isolation between closely related species, which is a driving force of speciation (Allison and Cardé, 2016; Roelofs et al., 2002).

The pheromone components of most moths are modified from the products of the normal fatty acid metabolism by a set of tissue-specific enzymes, including desaturases, fatty acyl reductases, aldehyde reductases, acetyl transferases, and acetate esterases (Ding and Löfstedt, 2015; Groot et al., 2016; Tillman et al., 1999). To identify the enzyme genes responsible for determining interspecific pheromone divergence, transcriptome sequencing of sex pheromone glands have been done in various moth species (Gu et al., 2013; Jung and Kim, 2014; Li et al., 2015; Strandh et al., 2008; Vogel et al., 2010; Xia et al., 2015; Zhang et al., 2014). So far, two classes of essential enzymes involved in the moth pheromone biosynthesis pathway, desaturases and fatty acyl reductases (FARs), have been found to account for pheromone differences between closely related moth species.

* Corresponding author. State Key Laboratory of Integrated Management of Pest Insects and Rodents, Institute of Zoology, Chinese Academy of Sciences, 1 Beichen West Road, Chaoyang District, Beijing, China.
E-mail address: czwang@ioz.ac.cn (C.-Z. Wang).

https://doi.org/10.1016/j.ibmb.2017.09.016
0965-1748/© 2017 Elsevier Ltd. All rights reserved.

Desaturases, functioning to introduce double bonds into pheromone precursors at various positions (Hao et al., 2002; Liénard et al., 2008; Liu et al., 2002, 2004; Matousková et al., 2007; Moto et al., 2004; Roelofs et al., 2002; Wang et al., 2010), are most intensively studied enzymes involved in sex pheromone biosynthesis (Knipple et al., 2002). In two *Ostrinia* species, Δ11-and Δ14-desaturases show alternate expression in the pheromone glands, with Δ11-desaturase expressed only in the pheromone gland of *O. scapulalis* while Δ14-desaturase only in that of *O. furnacalis* (Sakai et al., 2009). Within the New Zealand endemic leafroller genera, *Ctenopseustis* and *Planotortrix*, differential expression of a Δ10 desaturase gene is responsible for the presence of Z8-14:OAc in their pheromone glands (Albre et al., 2012).

Fatty acyl reductases (FARs) catalyze reduction of fatty acids to alcohols in the pheromone biosynthesis pathway. Alcohols can be pheromone components themselves or converted to aldehydes or acetate esters (Groot et al., 2016; Jurenka, 2003, 2004). The FAR orthologs in eight *Ostrinia* species exhibit different substrate specificities in converting acyl precursors into fatty alcohols, which result in differences in pheromone composition among *Ostrinia* congeners (Lassance et al., 2013).

The sympatric closely related species, *Helicoverpa armigera* and *Helicoverpa assulta*, use Z11-16:Ald and Z9-16:Ald as their principal sex pheromone components but in opposite ratios, 97: 3 in *H. armigera* and 7: 93 in *H. assulta*. Besides, Z11-16:OH, Z9-16:OH, Z11-16:OAc and Z9-16:OAc are abundant in the pheromone gland of *H. assulta* but not in that of *H. armigera* (Cork et al., 1992; Kehat and Dunkelblum, 1990; Liu et al., 2008; Park et al., 1996; Wu et al., 1997). The regulatory mechanisms underlying such species-specific ratios have been a central interest in understanding of the pheromone-based reproductive isolation between the two closely-related species.

Previous labeling experiments and GC-MS analysis have demonstrated that Δ11 desaturase is the sole desaturase for the production of the two pheromone components in *H. armigera*. In *H. assulta,* by contrast, Δ9 desaturase is the major desaturase responsible for biosynthesis of the major component Z9-16:Ald, whereas Δ11 desaturase is responsible for production of the minor component Z11-16:Ald (Wang et al., 2005). Moreover, the top three abundantly-expressed desaturase genes of *H. assulta* have been functionally characterized *in vitro* (Jeong et al., 2003). The most abundant one is *NPVE,* which encodes a Δ9 desaturase producing more Z9-18:Acid than Z9-16:Acid; the next one is *KPSE,* which also encodes a Δ9 desaturase but producing more Z9-16:Acid than Z9-18:Acid; and the third desaturase gene is *LPAQ,* which encodes a Δ11 desaturase producing only Z11-16:Acid (Jeong et al., 2003). Because *NPVE* and *KPSE* are responsible for the production of Z9-16:Ald and *LPAQ* is responsible for the production of Z11-16:Ald, we expect significantly higher expression of *NPVE* and *KPSE* in *H. assulta* and greater expression of *LPAQ* in *H. armigera*. Partially contradictory to this speculation, *NPVE* expresses at the highest level in pheromone glands of both *H. armigera* and *H. assulta* (Li et al., 2015). Therefore, it remains unclear which desaturase genes account for the opposite Z11-16:Ald/Z9-16:Ald ratio in the two *Helicoverpa* species. Another unanswered question is the molecular basis of their difference in the abundance of alcohols and acetate esters.

To address the two questions, we first conducted RNA-seq and qRT-PCR to elucidate the expressional divergence of the candidate enzyme genes involved in the pheromone biosynthetic pathway between the two *Helicoverpa* species. We then set up a number of cross-species hybridizations and backcrosses of F1 hybrids with *H. assulta* to generate backcross offspring, which should have a genotype of either heterozygous (*H. armigera/H. assulta*) or homozygous (*H. assulta/H. assulta*) at each of those expressional divergence loci, and thus variable levels of the two pheromone components and of the transcripts of the divergence loci. Finally, we simultaneously carried out GC-MS analysis of the two pheromone components and qRT-PCR analysis of the identified divergently-expressed genes in single pheromone glands of the backcross offspring. The data obtained demonstrate that the expressional divergences of *LPAQ* and *NPVE* leads to the opposite Z11-16:Ald/Z9-16:Ald ratios in the two species, whereas the expressional divergences of *FAR1* and *AR3* may account for the greater alcohol accumulation in *H. assulta*'s pheromone glands.

2. Materials and methods

2.1. Insects and crosses

H. armigera and *H. assulta* were originally collected as larvae in tobacco fields in Zhengzhou, Henan province of China, and successive generations were maintained in the laboratory under a 16 L: 8D photoperiod cycle at 26 ± 1 °C and 55–65% relative humidity. The larvae were reared on the wheat germ artificial diets (Wu et al., 2013). Pupae were sexed and males and females were put into separate cages for eclosion. After emergence, moths were fed with 10% honey water. Two to three-day old virgin females were used in the experiments.

Fifty couples of female *H. armigera* and male *H. assulta* (RS cross) and 50 of male *H. armigera* and female *H. assulta* (SR cross) were set up in cylindrical cages (diameter 28 cm, height 35 cm) separately to get RS and/or SR F1 hybrids. But we only got RS hybrids. Backcross offsprings (BC1) were obtained by crossing RS F1 males with female *H. assulta* (Xu et al., 2016). The hybrids were reared under the same conditions as their parental species.

2.2. Library construction and illumina sequencing

One hundred pheromone glands together with ovipositors were dissected out from virgin female *H. armigera* or *H. assulta* during the 5th-8th hour of the scotophase. To make sure that the insects are from the right species, we put each pupa in one tube and carefully verified their identity just after emergence. They were pooled and stored in −80 °C freezer until RNA extraction. Total RNA was isolated using RNeasy Plus Universal Mini Kit (Qiagen, Hilden, Germany) and potential genomic DNA contaminants were removed by gDNA Eliminator. RNA concentration was determined using a ND-2000 spectrophotometer (Nanodrop, Wilmington, DE, USA). RNA integrity was verified on Agilent 2100 BioAnalyzer (Agilent, USA).

mRNA was isolated from ten μg of total RNA by magnetic beads with Oligo (dT) using Dynabeads® mRNA purification kit (Invitrogen, USA). The resultant mRNA was used to construct paired-end RNA-seq libraries following the Illumina's library construction protocol. To avoid sample contaminations, we performed all the RNA isolations and library constructions in our laboratory. The libraries were sequenced on Illumina HiSeq2000 platform (Illumina, USA) in the Beijing Institutes of Biological Sciences (Chinese Academy of Sciences). FASTQ files of raw-reads were produced and sorted out by barcodes for further analysis.

2.3. Assembly of transcriptomes and gene identification

Prior to assembly, 2 × 100 bp paired-end raw reads from each cDNA library were processed to remove adaptors, low quality sequences (Q < 20), and reads contaminated with microbes using Trimmomatic package (Bolger et al., 2014). The FastQC package was used to verify the quality of the resulting trimmed and filtered reads. The clean reads obtained were *de novo* assembled to contigs using the default parameters of the short reads assembling

program Trinity. One set of transcript contigs was assembled from the clean reads of each library. The expression level of each contig, i.e. FPKM (fragments per kilobase of exon per million fragments mapped) value, was calculated using the RSEM package.

We downloaded the amino acid sequences of desaturases, fatty acyl reductases, aldehyde reductases, acetyl transferases, and acetate esterases of Lepidopteran insects from NCBI to construct the corresponding local databases. We used these local databases as the queries to BlastX search against the assembled transcriptome database with an E-value cut-off of 1e−5 to identify the putative genes involved in the sex pheromone biosynthesis pathway. The identified putative genes were verified by BlastX search against the NCBI Nr database. The open reading frames (ORFs) of the putative genes were predicted by using ORF finder (http://www.ncbi.nlm.nih.gov/gorf/gorf.html).

The sequence reads data of 8 *H. armigera* tissues (larval antennae, larval fat bodies, male adult heads, Duplex-Specific thermostable nuclease (DSN) treated male adult heads, female adult heads, DSN treated female adult heads, female adult tarsi and female abdomens) were downloaded from NCBI sequence read archive (SRA) (http://www.ncbi.nlm.nih.gov/sra/?term=SRP041166; Liu et al., 2014). The SRA Toolkit was used to convert the data to fastq format. The reads data of the above 8 tissues and those of the pheromone glands and larvae maxillary we sequenced were trimmed using Trimmomatic-0.30, merged, assembled using Trinityrnaseu-r2013-02-25, redundancy-removed using Tgicl, and finally capped using Cap3 to a large collection of *H. armigera* unigenes (Ning et al., 2016). The detailed information of the transcriptome data used in this study is available in Table S3. The FPKM value of every candidate gene in different tissues was calculated using the RSEM package.

In addition to sequencing *H. assulta* pheromone gland transcriptome, we also sequenced the transcriptomes of four other *H. assulta* tissues (male antennae, female antennae, proboscis, and forelegs). Using the same procedure described above for assembly of the reads data of the 10 *H. armigera* tissues, we merged and assembled the 5 *H. assulta* tissue transcriptome data into a large collection of *H. assulta* unigenes and calculated the FPKM values of the identified candidate genes in the 5 tissues.

2.4. Sequence verification of identified genes from transcriptome sequencing

RT-PCR cloning and sequencing were used to verify authentication of the identified genes. The total RNAs were isolated from pheromone gland using RNeasy Mini Kit (Qiagen, Hilden, Germany) and then reverse transcribed to cDNA by using MMLV reverse transcriptase (Promega, Madison, WI, USA). PCR experiments were conducted in a 25 μL reaction system with Q5® High-Fidelity DNA Polymerase (NEB) by using a ABI PCR machine. Primers were designed using Primer Premier 5.0 software (PREMIER Biosoft International) and the sequences were available in Table S1. The thermal cycling conditions were set as follows: 98 °C for 30 s; 30 cycles of 98 °C for 10 s, 50 °C for 30 s, and 72 °C for 90 s; and 72 °C for 2 min. PCR products were analyzed on 1.2% agarose gels and purified by MiniBEST Agarose Gel DNA Extraction Kit (Takara, Dalian, China). Then they were ligated into pGEM-T easy vectors (Promega, Madison, WI, USA). TOP10 competent cells (Tiangen, Beijing, China) were transformed with the ligation products, positive clones were grown in LB medium containing ampicillin. Five positive clones of each gene were selected and sequenced (Sino-GenoMax company, Beijing, China). Primers for qPCR analysis were designed according to the sequencing results.

2.5. Alignment and phylogenetic analysis of putative desaturases

Amino acid sequence alignments of *H. armigera* and *H. assulta* desaturase were carried out using ClustalW program (Thompson et al., 1994). Phylogenetic relationships among *H. armigera* and *H. assulta* desaturases were inferred by Neighbor-Joining analysis (Saitou and Nei, 1987) in MEGA5.2.

2.6. Quantitative RT-PCR (qRT-PCR)

The head, thorax, abdomen, legs, wings, and pheromone gland (with no ovipositor) of the female *H. armigera* and *H. assulta* were dissected for RNA extraction separately. cDNA was synthesized with M-MLV reverse transcriptase (Promega, Madison, WI, USA) from the total RNA. Real-time PCR were carried out using Mx3005P qPCR System (Agilent Technologies, CA, USA). The primer sequences are listed in Table S1. All reactions were performed in triplicate in a total volume of 20 μL containing 10 μL SYBR Premix Ex TaqII (Takara, Dalian, China) and 0.4 mM of each primer under the following conditions: 95 °C for 30 s followed by 40 cycles of 95 °C for 5 s, 60 °C for 34 s, and 72 °C for 30 s, 1 cycle 95 °C for 15s, 60 °C for 1 min, 95 °C for 15 s. Expression levels of all detected genes were calculated using the $2^{-\Delta Ct}/2^{-\Delta Ct\Delta Ct}$ method, with 18S gene transcript as an internal control for sample normalization. All experiments were repeated three times using three independent RNA samples.

2.7. GC-MS analysis

The single pheromone gland with no ovipositor (PG) of 14 2- to 3-day-old backcross female offspring (BC1 family) were individually dissected at 5–7 h into the scotophase and individual PGs were extracted for 15 min at room temperature in 7 μL hexane contained in a 300-μL insert placed in a 2-mL screw-cap vial (Agilent Technologies, CA, USA). Two microliters of the hexane extract were injected into an Agilent 6890 Series gas chromatograph, in the scan mode using an Agilent 5973N mass selective detector. The sex pheromone components were separated on a DB-Wax polyethylene glycol capillary column (60 m × 250 μm × 0.25 μm) using helium as a carrier gas, with an inlet pressure of 12 psi. The oven temperature was held at 50 °C for 1 min, followed by an increase of 10 °C/min to 180 °C, 3 °C/min to 220 °C and then held for 5 min. Peaks were identified by comparison with the Z9-16:Ald and Z11-16:Ald standards. The ratio of Z9-16:Ald's peak area to Z11-16:Ald's peak area was calculated to represent the relative proportion of Z9-16: Ald. The relative proportion of Z11-16: Ald was calculated by the same manner (Z11-16:Ald's peak area to Z9-16:Ald's peak area).

The single pheromone glands used for GC analyses were re-used for RNA extraction and qPCR analyses in order to examine the relationship between the proportion of the sex pheromone components and the level of expression of individual desaturases in the same pheromone glands (Albre et al., 2013). To measure expression levels correctly, the qRT-PCR primers were designed from the conserved regions of *H. armigera* and *H. assulta* desaturase genes.

2.8. RNAi

Double-stranded RNAs (dsRNA) were synthesized with the T7 RiboMAX Express RNAi system (Promega, Madison, USA), following the manufacturer's instructions. The concentration of dsRNA was determined with an ND-2000 spectrophotometer. The quality was verified by 1.2% agarose gel electrophoresis. The final

concentrations of dsRNA were adjusted to 5 μg/μL. Four microliter of ds*HarmLPAQ* (20 μg), or 4 μL of nuclease-free water (blank control) was injected into the tip of the abdomen of female *H. armigera* pupa at the eighth day after pupation (one day before eclosion). Subsequently, the injected pupae were marked and returned to the mass-rearing cages. Seventy two hours post emergence, the sex pheromone gland of every single injected moth was dissected out and employed to measure its Z11-16:Ald/Z9-16:Ald ratio and abundance of *HarmLPAQ* transcript using the GC-MS and qRT-PCR analyses described above. To avoid the disturbance of off-target effects, the qPCR primers were designed to detect the flanking region of the dsRNA fragment.

3. Results

3.1. Transcriptome sequencing and identification of putative genes involved in sex pheromone biosynthesis

We carried out RNA-seq of the female pheromone glands/ovipositors of *H. armigera* and *H. assulta* separately using the Illumina HiSeq(TM) 2000 platform. Approximately 39 (3.9 Gb) and 49 (4.9 Gb) million sequence reads were obtained from *H. armigera* and *H. assulta* pheromone/ovipositor tissues, respectively. After clustering and redundancy filtering, we acquired 53435 *H. armigera* unigenes with an N50 length of 1238 bp and 53628 *H. assulta* unigenes with an N50 length of 1671 bp. BlastX searches against the yielded *H. armigera* and *H. assulta* sex pheromone gland unigene databases using the amino acid sequences of the lepidopteran sex pheromone synthesis genes downloaded from NCBI as the queries identified a total of 90 (GenBank accession number: MF687523-MF687581, MF706167-MF706196, MF740790) and 86 (MF687582- MF687667) sex pheromone production related enzyme genes from *H. armigera* and *H. assulta* respectively (Table S2). These include desaturases, fatty acyl reductases, aldehyde reductases, acetyl transferases and acetate esterases.

3.2. Abundances and tissue expression patterns of sex pheromone biosynthesis genes in the two species

Desaturases Nine and 8 desaturase genes were identified in the pheromone glands of *H. armigera* and *H. assulta*, respectively. Based on a motif of four amino acids at positions 165–168 (Knipple et al., 2002), the 17 desaturases were divided into 9 subgroups and named as *LPAQ, NPVE, KPSE, GATD, MPVE, PDSN, KSVE, QPGE*, and *IPAE*, respectively (Fig. 1A). Consistent with this motif-based classification, phylogenetic analysis resolved the 17 desaturases into 8 ortholog pairs and 1 IPAE from *H. armigera* (named *HarmIPAE*) (Fig. 1B). *HarmLPAQ* expressed most abundantly (4964.37 FPKM) in *H. armigera* pheromone gland, whereas *HassNPVE* showed a super high expression level (15718.49 FPKM) in *H. assulta* pheromone gland. All the other desaturase genes had a much lower expression level than *HarmLPAQ* in *H. armigera* and than *HassNPVE* in *H. assulta* (Fig. 2A).

qRT-PCR results confirm that in *H. armigera* pheromone gland, the expression level of *HarmLPAQ* is about 30 times higher than that of *HarmNPVE,* 210 times higher than that of *HarmKPSE* (Fig. 3A1), while in *H. assulta* pheromone gland, the expression level of *HassNPVE* is about 79 times higher than that of *HassKPSE*, and 136 times higher than that of *HassLPAQ* (Fig. 3B1). The three desaturases show different tissue expression specificity in the two species (Fig. 3, Fig. 4A). In *H. armigera*, *HarmLPAQ* is expressed predominantly in the pheromone gland, and *HarmNPVE* and *HarmKPSE* have much lower expressions in the pheromone gland, even lower than in some other tissues such as the female adult thorax and abdomen (Fig. 3A, Fig. 4A1). In *H. assulta*, *HassNPVE* is expressed predominantly in the pheromone gland, and *HassLPAQ* and *HassKPSE* show higher expressions in the pheromone gland than in other tissues (Fig. 3B, Fig. 4A2). It is worth mentioning that *HarmQPGE* expressed very low in the pheromone gland of *H. armigera* but abundantly in larval fat body (Fig. 4A1).

Fatty acyl-CoA reductases (FAR) Sixteen and twelve putative FAR genes were expressed in the pheromone glands of *H. armigera* and *H. assulta,* respectively. *FAR1* orthologs (*HarmFAR1*, 1039.34 FPKM; *HassFAR1,* 937.16 FPKM) from two species had the highest mRNA abundance level among the identified *FAR* genes (Fig. 2B). Both *HarmFAR1* and *HassFAR1* were predominantly expressed in pheromone gland (Fig. 4B).

Alcohol Oxidases (AO) There were 4 and 5 alcohol oxidases in the pheromone gland transcriptomes of *H. armigera* and *H. assulta*, respectively. Both *HarmAO1* (762.351 FPKM) and *HassAO1* (909.99 FPKM) exhibited the highest expression level among the alcohol oxidase genes (Fig. 2C). *HarmAO1* and *HassAO1* displayed much higher expression level in the pheromone gland than other tissues (Fig. 4C).

Aldehyde reductases (AR) Among the 12 aldehyde reductases in the pheromone gland of *H. armigera* and *H. assulta*, *HarmAR1* (134.65 FPKM) and *HassAR3* (106.63 FPKM) showed the highest expression level, respectively (Fig. 2D). *HarmAR1* was also highly

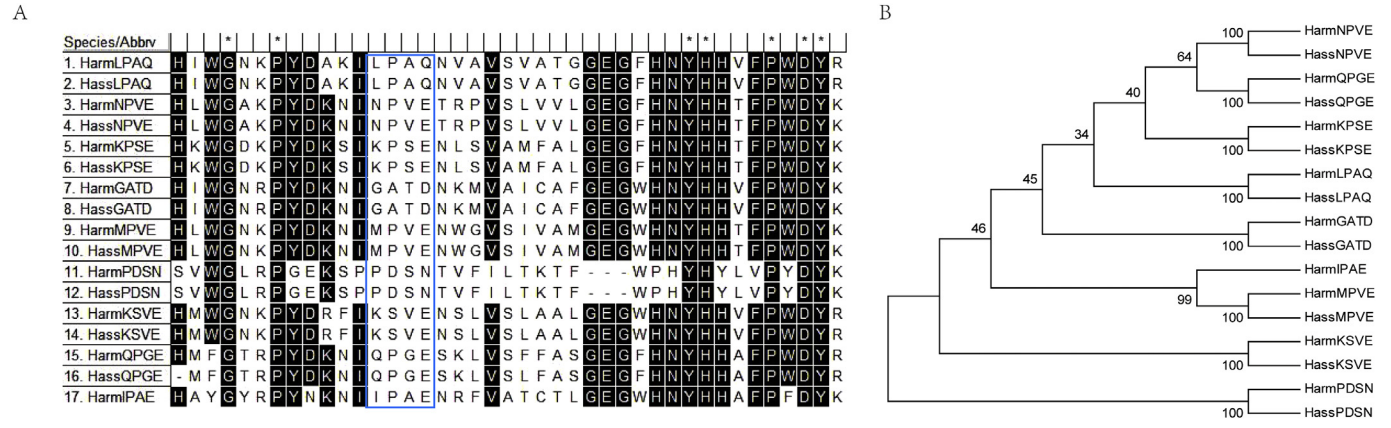

Fig. 1. Alignment and phylogenetic analysis of putative desaturases. (A) The amino acid sequence alignment of desaturases of *H. armigera* and *H. assulta*. The signature motifs of these genes are framed out. The amino acids identical in all the aligned sequences are marked with an asterisk. Residues shared among most of desaturase sequences are shown in white typing on a black background. (B) The phylogenetic tree is constructed with MEGA5.2 using the neighbor-joining method. Values shown next to the branches are results of bootstrap with 1000 replicates.

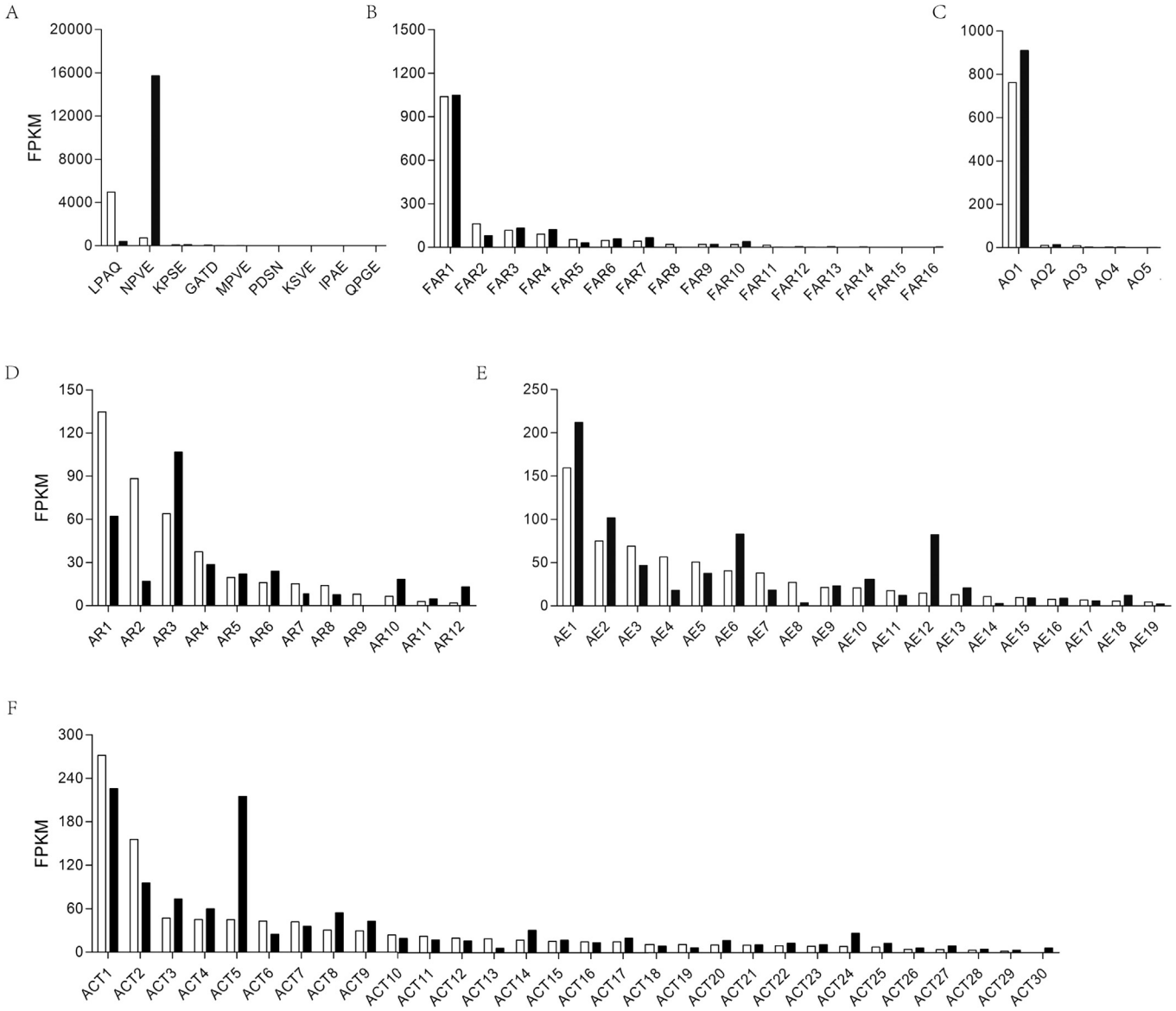

Fig. 2. FPKM of the pheromone biosynthesis related genes in the complex of pheromone glands and ovipositors of *H. armigera* (white column) and *H. assulta* (black column) showing in ortholog pairs. (A) desaturases, (B) fatty acyl reductases, (C) alcohol oxidases, (D) aldehyde reductases, (E) acetate esterases, (F) acetyl transferases.

expressed in larval maxilla, while *HassAR1* had a much higher expression level in female forelegs. *HassAR3* showed a higher expression level in pheromone gland than other *H. assulta* tissues examined. *HassAR6* was abundantly expressed in the male antennae (Fig. 4D), implicating a role in pheromone degradation.

Acetyltransferases (ACT) In the pheromone gland transcriptome of *H. armigera* and *H. assulta*, 30 putative acetyltransferase (*ACT*) genes were identified. *HarmACT1* (271.59 FPKM) had much more transcripts than the other 29 *H. armigera ACT* genes in the pheromone gland, while its *H. assulta* ortholog *HassACT1* (225.53 FPKM) had a similar level of expression with *HassACT5* (215.05 FPKM), both of which showed much higher abundances than the other 28 *H. assulta ACT* genes in the pheromone gland (Fig. 2E). Among the examined tissues of *H. armigera*, *HarmACT1* had the highest expression level in the pheromone gland. *HassACT1* displayed a high expression level in the pheromone gland and the male antennae. *HassACT5* was expressed predominantly in the pheromone gland, while *HarmACT5* was not (Fig. 4E).

Acetate esterase (AE) A total of 19 putative acetate esterase genes were identified from the pheromone glands of either *H. armigera* or *H. assulta*. The orthologs *HarmAE1* (155.37 FPKM) and *HassAE1* (211.93 FPKM)were the most abundantly expressed acetate esterase genes in the two species (Fig. 2F). *HarmAE1* is also known as *HarmCCE025a*, but its potential function is still unknown (Teese et al., 2010). Both *HarmAE1* and *Hass AE1* showed much higher expression in the pheromone gland than the other tissues (Fig. 4F), indicating their role in degrading acetate esters in both species. Moreover, *HassAE12* transcript was more abundant in the pheromone gland than the other tissues. *HassAE2*, *HassAE6* and *HassAE7* exhibited an antennae-biased expression pattern (Fig. 4F).

3.3. Comparison of the expression levels of ten sex pheromone biosynthesis genes between the two species

The expression levels of ten pairs highly expressed or specifically expressed sex pheromone biosynthesis enzyme genes (*LPAQ*,

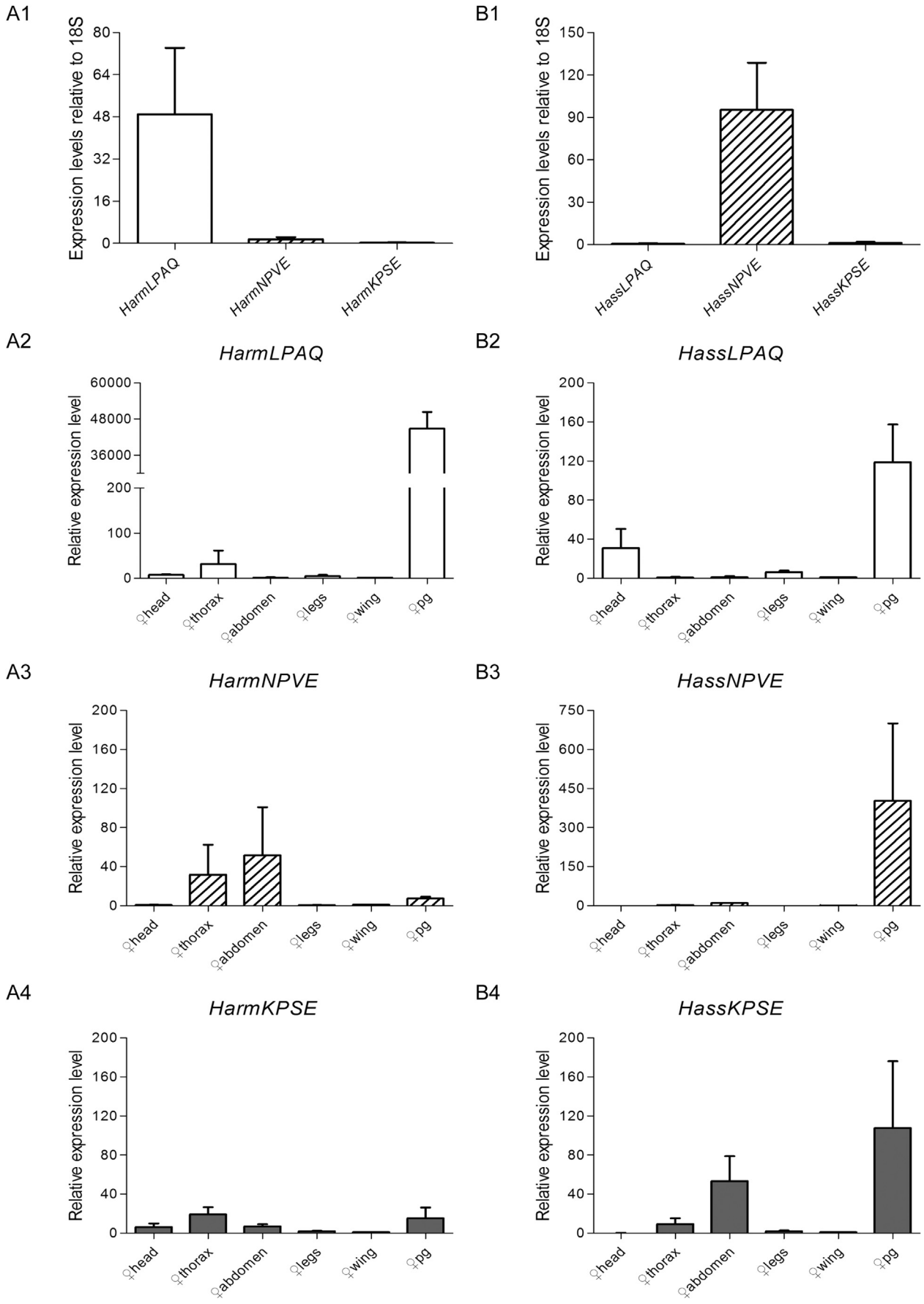

Fig. 3. The expression patterns of three desaturase genes, *LPAQ*, *NPVE* and *KPSE* in the pheromone gland and other tissues of *H. armigera* and *H. assulta*. (A1, B1) The expression levels of *LPAQ*, *NPVE* and *KPSE* in the pheromone gland of *H. armigera* and *H. assulta*; the expression level of each gene is calculated relative to the control gene 18S by using the $2^{-\Delta Ct}$ method. (A2-4, B2-4) The tissue expression patterns of *LPAQ*, *NPVE* and *KPSE* in *H. armigera* and *H. assulta*, the expression level of each gene is calculated using the $2^{-\Delta\Delta Ct}$ method (the expression level in the wing as the calibrator). The relative expression level is indicated as mean ± SEM (N = 3). All tissues tested were collected from the female moths. pg, pheromone gland.

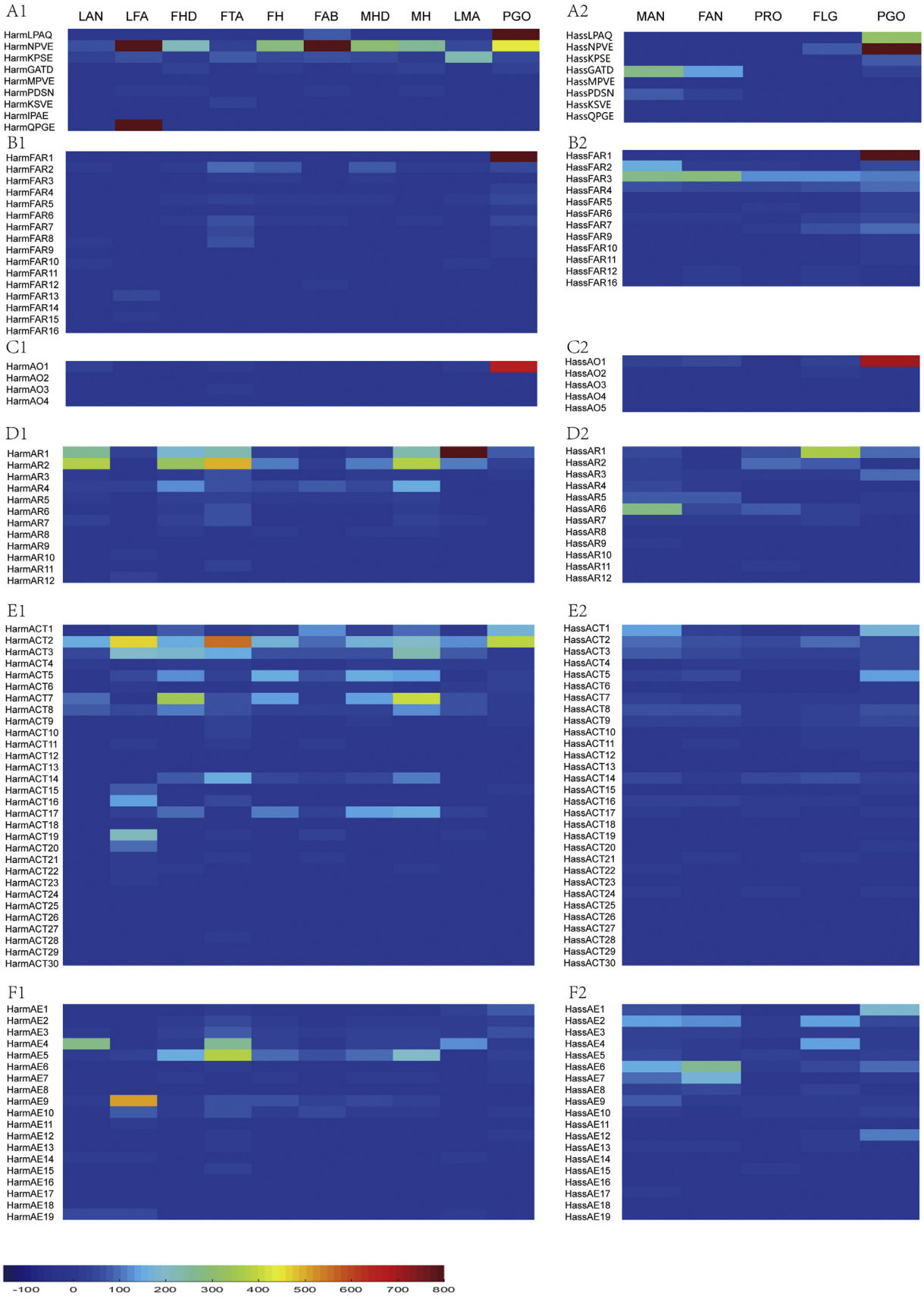

Fig. 4. Development- and tissue-expression profiles of the related enzyme genes in the pheromone biosynthesis of *H. armigera* (Harm) and *H. assulta* (Hass). (A1, A2) desaturases, (B1, B2) fatty acyl reductases, (C1, C2) alcohol oxidases, (D1, D2) aldehyde reductases, (E1, E2) acetyl transferases, (F1, F2) acetate esterases. LAN, larval antennae; LFA, larval fat bodies; FHD, DSN treated female adult heads; FTA, female adult tarsi; FH, female adult heads; FAB, female abdomens; MHD, DSN treated male adult heads; MH, male adult heads; LMA, larval antennae and maxillae; PGO, female pheromone glands and ovipositors; MAN, male antennae; FAN, female antennae; PRO, mixed female and male proboscis; FLG, mixed female and male forelegs.

NPVE, *KPSE*, *FAR1*, *AR3*, *AO1*, *ACT1*, *ACT5*, *AE1*, and *AE12*) identified above were compared between the two species further by qRT-PCR.

HarmLPAQ expressed about 70 times higher than *HassLPAQ*, while *HassNPVE* expressed about 60 times higher than *HarmNPVE* (Fig. 5A). *HassFAR1* expressed approximately 7 times higher than *HarmFAR1* (Fig. 5B); and *HassAR3* expressed approximately 280 times higher than *HarmAR3* (Fig. 5B). However, the other six genes, including *KPSE*, *AO1*, *ACT1*, *ACT5*, *AE1*, and *AE12*, displayed no significant differences in the expression level between the two species (Fig. 5B).

3.4. Positive correlation between the LPAQ or NPVE expression and the ratio of Z11-16: Ald and Z9-16: Ald

RNAi-based knockdown and cross-species hybridization experiments were conducted to verify the roles of the divergently-expressed *LPAQ* and *NPVE* desaturase genes in determining the opposite ratio of the two main pheromone components *in vivo*. Injection of *LPAQ* or *NPVE* dsRNA failed to effectively knockdown the two target genes in most of the dsRNA-injected *H. armigera* or *H. assulta* individuals (Data in Fig. S1) and thus yielded no useful data to support their roles in determining the Z11-16: Ald/Z9-16: Ald ratio. Fortunately, our cross-species hybridization experiment produced F1 (RS hybrids) and backcross offspring (BC1 family) derived from crossing F1 (RS male) with female *H. assulta* (Xu et al., 2016). Simultaneous analysis of the two sex pheromone components and the expression levels of *LPAQ* and *NPVE* in the pheromone gland of each of 14 BC1 females showed a wider range of individual variability in the abundances of Z11-16: Ald, Z9-16:Ald, *LPAQ* transcript, and *NPVE* transcript (Fig. 6). Eight out of the 14 BC1 females (BC1 individual 1-8 in Fig. 6A) produced more Z11-16: Ald than Z9-16:Ald, yielding a Z11-16: Ald/Z9-16: Ald ratio (Z11/Z9 ratio) of 2:1 to 5:1 (Fig. 6A). These 8 BC1 females also had a small NPVE/LPAQ ratio (the relative expression level of NPVE to LPAQ) (Fig. 6B). By contrast, the remaining 6 BC1 individuals (9-14 in Fig. 6A), had a much higher NPVE/LPAQ ratio (Fig. 6B), and thus synthesized more Z9-16:Ald than Z11-16: Ald, yielding a Z11/Z9 ratio of 1:12 to 1:49 (Fig. 6A). Further correlation analysis uncovered a linear positive correlation between the expression level of *LPAQ* and the relative production of Z11-16: Ald ($r^2 = 0.8305$, $P < 0.0001$) (Fig. 6C), and between the expression level of *NPVE* and the relative production of Z9-16: Ald ($r^2 = 0.4791$, $P = 0.0061$) although this positive correlation was gone when removing the putative outlier ($r^2 = 0.1164$, $P = 0.2540$) (Fig. 6D).

4. Discussion

It is well known that *H. armigera* produces 97:3 of Z11-16:Ald and Z9-16:Ald (aldehydes), little fatty acyl alcohols (Z11-16:OH and Z9-16:OH) and no acetate esters (Z11-16:Ac and Z9-16:Ac) in the sex pheromone gland, whereas its closely related species *H. assulta* synthesizes 7:93 of Z11-16:Ald and Z9-16:Ald and significant amounts of Z11-16:OH, Z9-16:OH, Z11-16:Ac and Z9-16:Ac. Such interspecies differences in the amounts of the 6 compounds are probably resulted from the divergent expression of certain genes involved in biosynthesis of these compounds between the two species. Transcriptomic comparisons and qRT-PCR analysis conducted in this study identified 4 pairs of orthologous genes that are divergently expressed in the sex pheromone glands of the two species. These include the Δ11-desaturase gene *LPAQ*, the Δ9-desaturase gene *NPVE*, the fatty acyl reductase gene *FAR1* and the aldehyde reductase gene *AR3*. Based on these differences and the previous studies (Hagström et al., 2012; Jeong et al., 2003; Wang et al., 2005), we propose the roles of these enzymes in the biosynthetic pathways for the principal pheromone components produced by female of *H. armigera* and *H. assulta* (Fig. 7). It is worth noting that in the biosynthetic process Z9-18:Acid could also be produced from 18:Acid through Δ9 desaturase in the pheromone gland of *H. assulta* which is not included in Fig. 7, and this leads to production of a small amount of Z7-16:Ald.

HarmLPAQ is the most abundantly expressed desaturase genes in *H. armigera*; and its transcripts are about 70 times more than those of its *H. assulta* ortholog *HassLPAQ*. On the contrary, *HassNPVE* is the most abundantly expressed desaturase genes in *H. assulta*; and its expression level is about 60 times higher than that of its *H. armigera* ortholog *HarmNPVE*. Li et al. (2015) reported that in both *H. armigera* and *H. assulta*, the expression of *NPVE* is the highest among the three desaturase genes (RPKM: *Harm*NPVE 4363.0, *Harm*LPAQ 3975.6, *Harm*KPSE 16.6; *Hass*NPVE 949.2, *Hass*KPSE 659.9, *Hass*LPAQ 132.9). The cause of this discrepancy is not clear, but our FPKM data are consistent with the results of qRT-PCR.

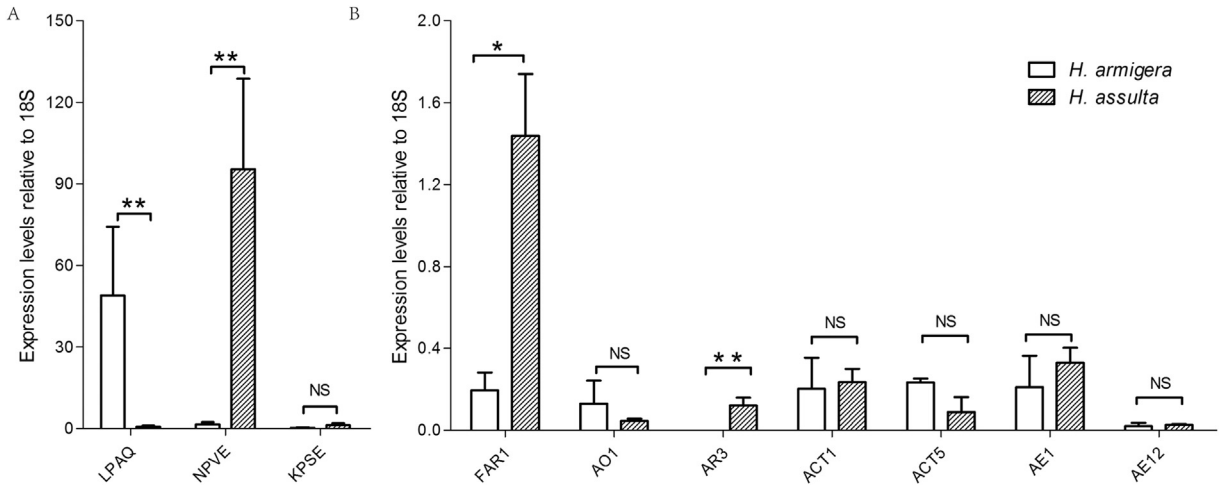

Fig. 5. Comparative analyses of the expression level of the selected genes in the pheromone glands of *H. armigera* and *H. assulta*. (A) desaturase (*LPAQ, NPVE* and *KPSE*), (B) the fatty acyl reductase (*FAR1*), the alcohol oxidase (*AO1*), the aldehyde reductase (*AR3*), the acetyl transferase (*ACT1* and *ACT5*), and the acetate esterases (*AE1* and *AE12*). The expression level (mean ± SEM, N = 3) of each gene is calculated relative to the control gene 18S by using the $2^{-\Delta Ct}$ method. One asterisk indicates significant difference between the two species ($P < 0.05$, Student's *t*-test); two asterisks indicate very significant difference ($P < 0.01$); NS indicates no significant difference ($P > 0.05$).

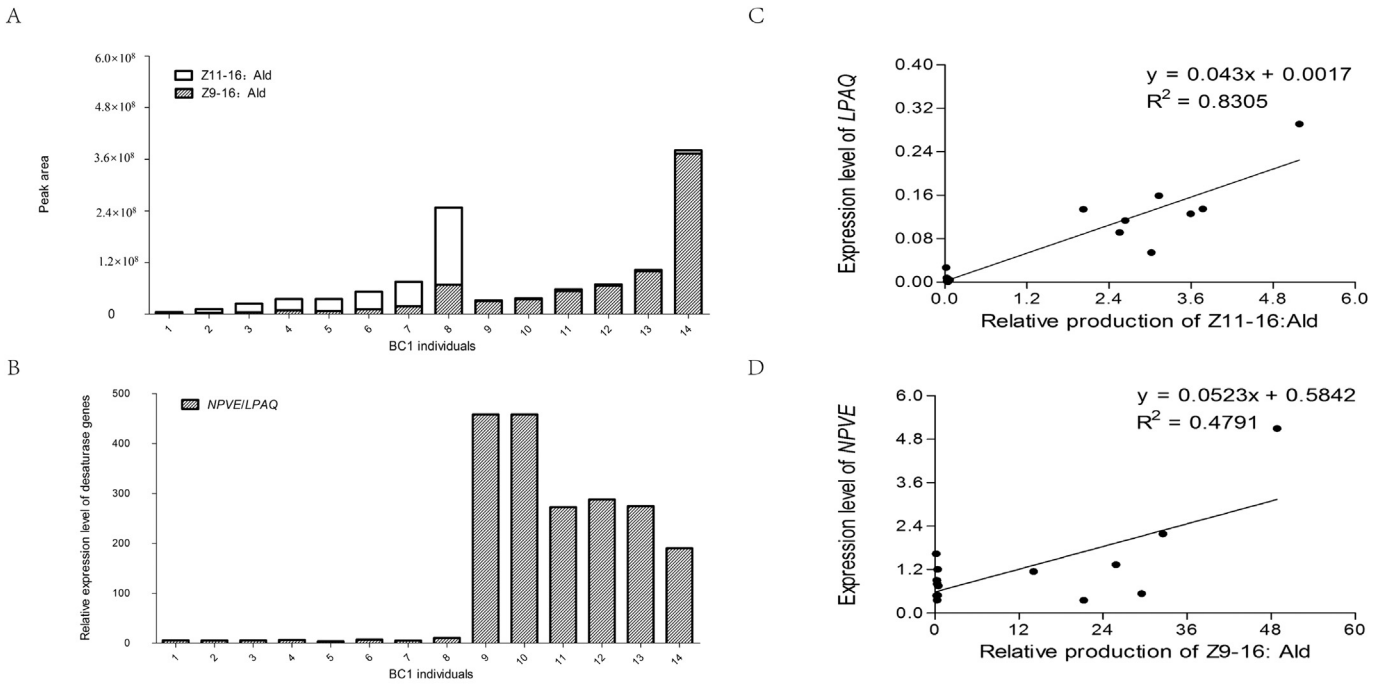

Fig. 6. Relationships between the relative production of two sex pheromone components and the expression level of the desaturases implicated in their biosynthesis from the same pheromone glands of BC1 progeny females (n = 14). (A) Z11-16:Ald/Z9-16:Ald ratio distribution of BC1 individuals. (B) The relative expression level of NPVE to LPAQ of BC1 individuals. (C) Correlation between the relative amount of Z11-16:Ald and the expression levels of LPAQ. (D) Correlation between the relative amount of Z9-16:Ald and the expression levels of NPVE.

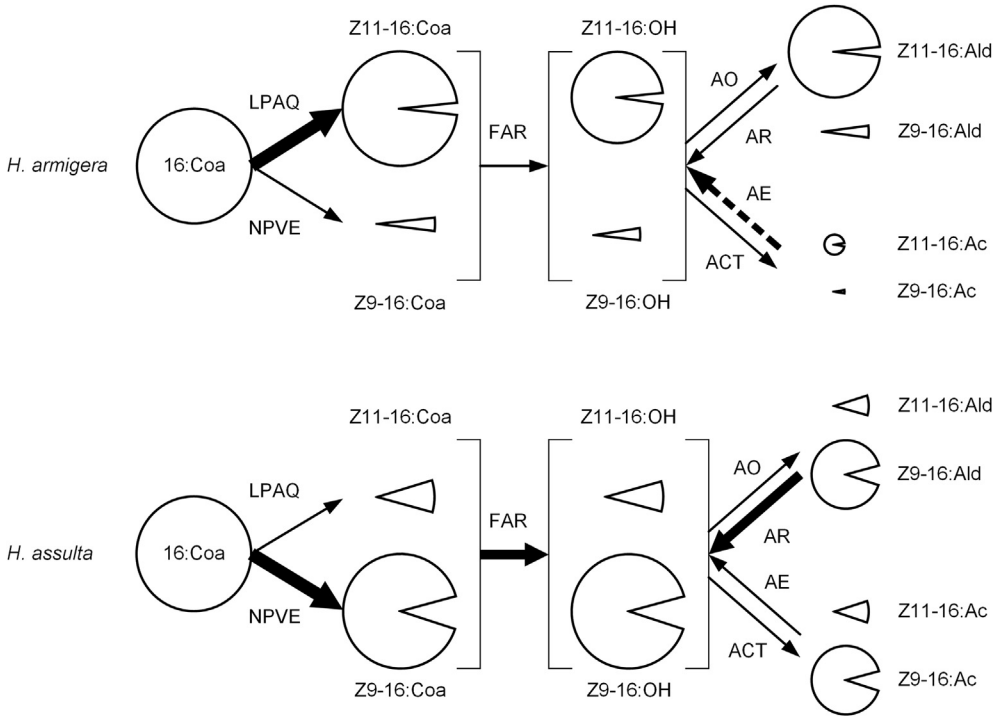

Fig. 7. Proposed biosynthetic pathways for the principal sex pheromone components produced by females of *H. armigera* and *H. assulta*. The area of the pie graphs indicates the relative amount of the substrates and products. The thickness of the arrows indicates the relative expression levels of the enzymes. The dotted arrow indicates a higher enzyme activity. FAR, fatty acyl reductases; AO, alcohol oxidases; AR, aldehyde reductases; ACT, acetyl transferases; AE, acetate esterases.

Our previous study show that in *H. assulta*, Δ9 desaturase and Δ11 desaturase act on palmitic acid to form Z9-16:Ald and Z11-16:Ald, respectively (Wang et al., 2005). Moreover, HassLPAQ is a Δ11-desaturase only producing Z11-16:Acid when expressed in a desaturase-deficient mutant yeast strain, while HassNPVE is a Δ9 desaturase producing more Z9-18:Acid than Z9-16:Acid (Jeong

et al., 2003). Consequently, our finding of higher expression of *HarmLPAQ* and lower expression of *HarmNPVE* in the pheromone gland of *H. armigera* is consistent with the production of 97:3 of Z11-16:Ald and Z9-16:Ald, whereas our finding of higher expression of *HassNPVE* in the pheromone gland of *H. assulta* and lower expression *HassLPAQ* is consistent with the production of 7:93 of Z11-16:Ald and Z9-16:Ald (Fig. 3). The fact that Z11-16: Ald and Z9-16: Ald production are positively correlated with the expression level of *LPAQ* and *NPVE,* respectively, in the BC1 female individuals further confirms that the expressional divergence of *LPAQ* and *NPVE* determine the opposite sex pheromone component ratios in the two species. However, the correlation of the expression level of *NPVE* with Z9-16: Ald production is not as strong as that of the expression level of *LPAQ* with Z11-16: Ald production. The possible reasons could be that (1) NPVE is not as specific in function as LPAQ in pheromone glands and may play other biological roles like in fatty acid metabolism and cold adaptation (Chen et al., 2014; Knipple et al., 2002), and (2) some other Δ9 desaturases like KPSE may also be involved in Z9-16: Ald production. It is always a confusing question which Δ9 desaturase, NPVE (more transcripts, 18:C preference) or KPSE (less transcripts, 16:C preference), plays a more important role in producing Z9-16:Ald in *H. assulta* (Jeong et al., 2003; Knipple et al., 2002). Considering its divergent expression patterns in the pheromone glands of the two species and the positive correlation between its expression levels and Z9-16:Ald production, we conclude that NPVE enzyme plays a vital role in producing Z9-16:Ald in *H. assulta.* In the pheromone gland of *H. assulta,* 16:Acid could be a major precursor and 18:Acid a minor one. The limited Z9-18:Acid generated by NPVE from 18:Acid may mainly transformed into Z7-16:Acid by β-oxidation immediately, and finally transformed into Z7-16:Ald as a minor sex pheromone gland component by reduction and oxidation (Wang et al., 2005).

The other two divergently expressed genes— the fatty acyl reductase gene *FAR1* and the aldehyde reductase gene *AR3*—are possibly involved in the production and/or conversion of alcohols (Z11-16:OH and Z9-16:OH), aldehydes (Z11-16:Ald and Z9-16:Ald) and acetate esters (Z11-16:Ac and Z9-16:Ac) (Fig. 7). In addition to fatty acyl reductase (FAR) and aldehyde reductase (AR); alcohol oxidases (AO), acetyltransferases (ACT) and acetate esterases (AE) are also involved in these processes (Fig. 7). As the common precursor of aldehydes and acetate esters, alcohols are catalyzed from CoA thioesters by FARs. Acetates esters are formed by adding an acetyl group to the unsaturated alcohols Z11-16:OH or Z9-16:OH by ACT, and can be converted back to alcohols by AE (Ding and Löfstedt, 2015; Fujii et al., 2010). Aldehydes are formed from alcohols by AO and can be converted back to alcohols by AR (Groot et al., 2016) (Fig. 7). Since HarmFAR1 and HassFAR1 have the similar reducing activity to catalyze Z9–14, Z9–16 and Z11–16:acyls into Z9-14:OH, Z9-16:OH and Z11-16:OH (Hagström et al., 2012), then the higher expression level of *HassFAR1* may lead to higher abundance of Z9-16:OH and Z11-16:OH in *H. assulta*. The higher expression of HassAR3 may be related to more Z9-16:Ald and Z11-16:Ald converting to Z9-16:OH and Z11-16:OH. This explains well why *H. assulta* has significantly higher accumulation of Z9-16:OH and Z11-16:OH in the pheromone gland than does *H. armigera.* However, the function of *AR3* in the pheromone biosynthesis of the two species needs to be further characterized.

In this study, we did not find significantly lower transcription of *H. armigera ACT* genes or higher transcription of *H. armigera AE* genes, both of which may result in un-detectability of acetate ester (Z9-16:Ac and Z11-16:Ac) in the sex pheromone gland of *H. armigera* (Fig. 7). However, significantly higher esterase (AE) activity was found in the pheromone gland of *H. armigera* than in the pheromone gland of *H. assulta* (Wang et al., 2008). This may account for the absence of acetate esters in the sex pheromone gland of *H. armigera*. The lack of difference in AE transcription suggests that the higher esterase activity in *H. armigera* than *H. assulta* may result from their divergence in the post-transcriptional, translational, and/or post-translational regulation/modifications of acetate esterases.

In conclusion, the opposite sex pheromone component ratios in *H. armigera* and *H. assulta* are largely regulated by the divergent expression of two desaturase genes, *LPAQ* and *NPVE,* in their pheromone glands. Interfering the expression of the two genes to disrupt the pheromone communication of *H. armigera* and *H. assulta* has great application potentials in pest management. The further study would focus on creating knockouts of pheromone production related enzyme genes by newly developed genome editing methods, like the CRISPR/Cas9 system.

Acknowledgements

We thank our colleagues Zhen Zou for his kind assistance in the transcriptome library construction, Xiao-Wei Qin, Rui Wang, Nan-Ji Jiang for their helps in GC-MS analysis and Rui Tang in data analysis. This work was supported by the National Key R&D Program of China (grant number 2017YFD0200400), National Natural Science Foundation of China (grant number 31471777 and 31130050), and USDA National Institute of Food and Agriculture (hatch grant ARZT-1360890-H31-164 and multi state grant ARZT-1370400-R31-168).

Appendix A. Supplementary data

Supplementary data related to this article can be found at https://doi.org/10.1016/j.ibmb.2017.09.016.

References

Albre, J., Liénard, M.A., Sirey, T.M., Schmidt, S., Tooman, L.K., Carraher, C., Greenwood, D.R., Löfstedt, C., Newcomb, R.D., 2012. Sex pheromone evolution is associated with differential regulation of the same desaturase gene in two genera of leafroller moths. PLoS Genet. 8, e1002489.

Albre, J., Steinwender, B., Newcomb, R.D., 2013. The evolution of desaturase gene regulation involved in sex pheromone production in leafroller moths of the genus planotortrix. J. Hered. 104, 627–638.

Allison, J.D., Cardé, R.T., 2016. Pheromones: reproductive isolation and evolution in moths. In: Allison, J.D., Cardé, R.T. (Eds.), Pheromone Communication in Moths. University of California Press, Oakland, California, pp. 11–23.

Bolger, A.M., Lohse, M., Usadel, B., 2014. Trimmomatic: a flexible trimmer for Illumina sequence data. Bioinforma. Oxf. Engl. 30, 2114–2120.

Chen, Q.M., Cheng, D.J., Liu, S.P., Ma, Z.G., Tan, X., Zhao, P., 2014. Genome-wide identification and expression profiling of the fatty acid desaturase gene family in the silkworm, *Bombyx mori*. Genet. Mol. Res. 13, 3747–3760.

Cork, A., Boo, K.S., Dunkelblum, E., Hall, D.R., Jee-Rajunga, K., Kehat, M., Kong Jie, E., Park, K.C., Tepgidagarn, P., Xun, L., 1992. Female sex pheromone of oriental tobacco budworm, *Helicoverpa assulta* (Guenee) (Lepidoptera: Noctuidae): identification and field testing. J. Chem. Ecol. 18, 403–418.

Ding, B.J., Löfstedt, C., 2015. Analysis of the *Agrotis segetum* pheromone gland transcriptome in the light of sex pheromone biosynthesis. BMC Genomics 16, 711.

Fujii, T., Ito, K., Katsuma, S., Nakano, R., Shimada, T., Ishikawa, Y., 2010. Molecular and functional characterization of an acetyl-CoA acetyltransferase from the adzuki bean borer moth *Ostrinia scapulalis* (Lepidoptera: Crambidae). Insect Biochem. Mol. Biol. 40, 74–78.

Groot, A.T., Dekker, T., Heckel, D.G., 2016. The genetic basis of pheromone evolution in moths. Annu. Rev. Entomol. 61, 99–117.

Gu, S.H., Wu, K.M., Guo, Y.Y., Pickett, J.A., Field, L.M., Zhou, J.J., Zhang, Y.J., 2013. Identification of genes expressed in the sex pheromone gland of the black cutworm *Agrotis ipsilon* with putative roles in sex pheromone biosynthesis and transport. BMC Genomics 14, 636.

Hagström, A.K., Liénard, M.A., Groot, A.T., Hedenström, E., Löfstedt, C., 2012. Semi-selective fatty acyl reductases from four heliothine moths influence the specific pheromone composition. PLoS One 7, e37230.

Hao, G., O'Connor, M., Liu, W., Roelofs, W.L., 2002. Characterization of Z/E11- and Z9-desaturases from the oblique banded leafroller moth, *Choristoneura rosaceana*. J. Insect Sci. 2, 26.

Jeong, S.E., Rosenfield, C.-L.L., Marsella-Herrick, P., Man You, K., Knipple, D.C., 2003. Multiple acyl-CoA desaturase-encoding transcripts in pheromone glands of *Helicoverpa assulta*, the oriental tobacco budworm. Insect Biochem. Mol. Biol. 33, 609–622.

Jurenka, R., 2003. Biochemistry of female moth sex pheromone. In: Blomquist, G.J., Vogt, R. (Eds.), Pheromone Biochemistry and Molecular Biology. Elsevier, London, pp. 107–136.
Jurenka, R., 2004. Insect pheromone biosynthesis. In: Schulz, S. (Ed.), Chemistry of Pheromones and Other Semiochemicals I (Topics in Current Chemistry). Springer-Verlag, Berlin, pp. 97–132.
Jung, C.R., Kim, Y., 2014. Comparative transcriptome analysis of sex pheromone glands of two sympatric lepidopteran congener species. Genomics 103, 308–315.
Kehat, M., Dunkelblum, E., 1990. Behavioral responses of male *Heliothis armigera* (Lepidoptera: Noctuidae) moths in a flight tunnel to combinations of components identified from female sex pheromone glands. J. Insect Behav. 3, 75–83.
Knipple, D.C., Rosenfield, C.-L.L., Nielsen, R., You, K.M., Jeong, S.E., 2002. Evolution of the integral membrane desaturase gene family in moths and flies. Genetics 162, 1737–1752.
Lassance, J.-M.M., Liénard, M.A., Antony, B., Qian, S., Fujii, T., Tabata, J., Ishikawa, Y., Löfstedt, C., 2013. Functional consequences of sequence variation in the pheromone biosynthetic gene pgFAR for *Ostrinia* moths. Proc. Natl. Acad. Sci. U.S.A. 110, 3967–3972.
Li, Z.Q., Zhang, S., Luo, J.Y., Wang, C.Y., Lv, L.M., Dong, S.L., Cui, J.J., 2015. Transcriptome comparison of the sex pheromone glands from two sibling *Helicoverpa* species with opposite sex pheromone components. Sci. Rep. 5, 9324.
Liénard, M.A., Strandh, M., Hedenström, E., Johansson, T., Löfstedt, C., 2008. Key biosynthetic gene subfamily recruited for pheromone production prior to the extensive radiation of Lepidoptera. BMC Evol. Biol. 8, 270.
Liu, M., Cai, J., Tian, Y., 2008. Sex pheromone components of the Oriental tobacco budworm, *Helicoverpa assulta* Guenee: identification and field trials. Insect Sci. 1, 77–85.
Liu, N.Y., Xu, W., Papanicolaou, A., Dong, S.L., Anderson, A., 2014. Identification and characterization of three chemosensory receptor families in the cotton bollworm *Helicoverpa armigera*. BMC Genomics 15, 597.
Liu, W., Jiao, H., O'Connor, M., Roelofs, W., 2002. Moth desaturase characterized that produces both Z and E isomers of Δ11-tetradecenoic acids. Insect Biochem. Mol. Biol. 32, 1489–1495.
Liu, W., Rooney, A.P., Xue, B., Roelofs, W.L., 2004. Desaturases from the spotted fireworm moth (*Choristoneura parallela*) shed light on the evolutionary origins of novel moth sex pheromone desaturases. Gene 342, 303–311.
Matousková, P., Pichová, I., Svatos, A., 2007. Functional characterization of a desaturase from the tobacco hornworm moth (*Manduca sexta*) with bifunctional Z11- and 10,12-desaturase activity. Insect Biochem. Mol. Biol. 37, 601–610.
Moto, K., Suzuki, M.G., Hull, J.J., Kurata, R., Takahashi, S., Yamamoto, M., Okano, K., Imai, K., Ando, T., Matsumoto, S., 2004. Involvement of a bifunctional fatty-acyl desaturase in the biosynthesis of the silkmoth, *Bombyx mori*, sex pheromone. Proc. Natl. Acad. Sci. U.S.A. 101, 8631–8636.
Ning, C., Yang, K., Xu, M., Huang, L.Q., Wang, C.Z., 2016. Functional validation of the carbon dioxide receptor in labial palps of *Helicoverpa armigera* moths. Insect Biochem. Mol. Biol. 73, 12–19.
Park, K.C., Cork, A., Boo, K.S., 1996. Intrapopulational changes in sex pheromone composition during scotophase in oriental tobacco budworm, *Helicoverpa assulta* (Guenée) (Lepidoptera: Noctuidae). J. Chem. Ecol. 22, 1201–1210.
Roelofs, W.L., Liu, W., Hao, G., Jiao, H., Rooney, A.P., Linn, C.E., 2002. Evolution of moth sex pheromones via ancestral genes. Proc. Natl. Acad. Sci. U.S.A. 99, 13621–13626.
Saitou, N., Nei, M., 1987. The neighbor-joining method: a new method for reconstructing phylogenetic trees. Mol. Biol. Evol. 4, 406.
Sakai, R., Fukuzawa, M., Nakano, R., Tatsuki, S., Ishikawa, Y., 2009. Alternative suppression of transcription from two desaturase genes is the key for species-specific sex pheromone biosynthesis in two *Ostrinia* moths. Insect Biochem. Mol. Biol. 39, 62–67.
Strandh, M., Johansson, T., Ahrén, D., Löfstedt, C., 2008. Transcriptional analysis of the pheromone gland of the turnip moth, *Agrotis segetum* (Noctuidae), reveals candidate genes involved in pheromone production. Insect Mol. Biol. 17, 73–85.
Teese, M.G., Campbell, P.M., Scott, C., Gordon, K.H., Southon, A., Hovan, D., Robin, C., Russell, R.J., Oakeshott, J.G., 2010. Gene identification and proteomic analysis of the esterases of the cotton bollworm, *Helicoverpa armigera*. Insect Biochem. Mol. Biol. 40, 1–16.
Thompson, J.D., Higgins, D.G., Gibson, T.J., 1994. CLUSTAL W: improving the sensitivity of progressive multiple sequence alignment through sequence weighting, position-specific gap penalties and weight matrix choice. Nucleic Acids Res. 22, 4673–4680.
Tillman, J.A., Seybold, S.J., Jurenka, R.A., Blomquist, G.J., 1999. Insect pheromones–an overview of biosynthesis and endocrine regulation. Insect Biochem. Mol. Biol. 29, 481–514.
Vogel, H., Heidel, A.J., Heckel, D.G., Groot, A.T., 2010. Transcriptome analysis of the sex pheromone gland of the noctuid moth *Heliothis virescens*. BMC Genomics 11, 29.
Wang, H.L., Liénard, M.A., Zhao, C.H., Wang, C.Z., Löfstedt, C., 2010. Neofunctionalization in an ancestral insect desaturase lineage led to rare Δ6 pheromone signals in the Chinese tussah silkworm. Insect Biochem. Mol. Biol. 40, 742–751.
Wang, H.L., Zhao, C.H., Wang, C.Z., 2005. Comparative study of sex pheromone composition and biosynthesis in *Helicoverpa armigera, H. assulta* and their hybrid. Insect Biochem. Mol. Biol. 35, 575–583.
Wang, H.L., Zhao, C.H., Yan, Y.H., Wang, C.Z., 2008. A comparative study on the conversion of alcohols and acetates in sex pheromone glands of *Helicoverpa armigera* and *H. assulta* (Lepidoptera: Noctuidae). Acta Entomol. Sin. 51 (9), 895–901.
Wu, D., Yan, Y., Cui, J., 1997. Sex pheromone components of *Helicoverpa armigera*: chemical analysis and field tests. Insect Sci. 4, 350–356.
Wu, H., Hou, C., Huang, L.Q., Yan, F.S., Wang, C.Z., 2013. Peripheral coding of sex pheromone blends with reverse ratios in two *Helicoverpa* species. PLoS One 8, e70078.
Xia, Y.H., Zhang, Y.N., Hou, X.Q., Li, F., Dong, S.L., 2015. Large number of putative chemoreception and pheromone biosynthesis genes revealed by analyzing transcriptome from ovipositor-pheromone glands of *Chilo suppressalis*. Sci. Rep. 5, 7888.
Xu, M., Dong, J.F., Wu, H., Zhao, X.C., Huang, L.Q., Wang, C.Z., 2016. The inheritance of the pheromone sensory system in two *Helicoverpa* species: dominance of *H. armigera* and possible introgression from *H. assulta*. Front. Cell Neurosci. 10, 302.
Zhang, Y.N., Xia, Y.H., Zhu, J.Y., Li, S.Y., Dong, S.L., 2014. Putative pathway of sex pheromone biosynthesis and degradation by expression patterns of genes identified from female pheromone gland and adult antenna of *Sesamia inferens* (Walker). J. Chem. Ecol. 40, 439–451.